AGU PUBLICATIONS

JGR

Journal of Geophysical Research: Earth Surface

RESEARCH ARTICLE

10.1002/2014JF003382

Key Points:
- Dependency of ground surface temperature histories on borehole depths
- Dependency of subsurface heat estimates on borehole depths
- Boreholes depth differences affect estimates of GSTH

Correspondence to:
H. Beltrami,
hugo@stfx.ca

Citation:
Beltrami, H., G. S. Matharoo, and J. E. Smerdon (2015), Impact of borehole depths on reconstructed estimates of ground surface temperature histories and energy storage, *J. Geophys. Res. Earth Surf.*, *120*, doi:10.1002/2014JF003382.

Received 31 OCT 2014
Accepted 26 MAR 2015
Accepted article online 10 MAR 2015

Impact of borehole depths on reconstructed estimates of ground surface temperature histories and energy storage

Hugo Beltrami[1,2], Gurpreet S. Matharoo[1], and Jason E. Smerdon[3]

[1]Climate and Atmospheric Sciences Institute and Department of Earth Sciences, St. Francis Xavier University, Antigonish, Nova Scotia, Canada, [2]Centre pour l'étude et la simulation du climat à l'échelle régionale, Université du Québec à Montréal, Montréal, Québec, Canada, [3]Lamont-Doherty Earth Observatory, Columbia University, Palisades, New York, USA

Abstract Estimates of ground surface temperature changes and continental energy storage from geothermal data have become well-accepted indicators of climatic changes. These estimates are independent contributions to the ensemble of paleoclimatic reconstructions and have been used for the validation of general circulation models, and as a component of the energy budget accounting of the global climate system. Recent global and hemispheric analyses of geothermal data were based on data available in the borehole paleoclimatology database, which contains subsurface temperature profiles from a minimum depth of 200 m to about 600 m. Because of the nature of heat conduction, different depth ranges contain the record of past and persistent changes in the energy balance between the lower atmosphere and the ground for different time periods. Here we examine the dependency of estimated ground surface temperature histories and the magnitude of the subsurface heat content on the depth of borehole temperature profiles. Our results show that uncertainties in the estimates of the long-term surface temperature are in the range of ±0.5 K. We conclude that previous estimates of ground surface temperature change remain valid for the period since industrialization, but longer-term estimates are subject to considerable uncertainties. The subsurface heat content shows a larger range of variability arising from differences in depth of the borehole temperature profiles, as well as from differences in the time of data acquisition, spanning four decades. These results indicate that estimates of subsurface heat should be carried out with caution to decrease cumulative errors in any spatial analysis.

1. Introduction

Global mean temperature increases and associated climate changes observed over the last 150 years, in addition to future projections of wide-ranging impacts due to continued human-induced climate change, underscore the urgency of concerted research efforts directed at understanding, quantifying, and explaining the mechanisms that drive climate variability and change over multiple timescales [*Beltrami*, 2002a; *Solomon*, 2007; *Jones et al.*, 2009; *Hansen et al.*, 2005, 2011, 2013; *Stocker et al.*, 2013; *Rhein et al.*, 2013]. General circulation models (GCMs) have become fundamental tools for exploring how and why the climate system has varied and changed in the past, as well as for quantifying the possible evolution of the climate system in the future under natural and anthropogenic pressures due to increasing concentrations of greenhouse gases [*Le Quéré et al.*, 2014]. Exploring GCM performance across a wide range of timescales and mean states is therefore a critical means of validating projected climate change risks in the future and understanding the dynamics of climate variability.

Recent attention on the so called "global warming hiatus" or the slowdown of the rate of increases in the global mean surface air temperature (SAT) has focused on the reasons underlying the inability of GCMs to more accurately represent SAT observations over the last two decades, which include explanations rooted in either climate variability or changes in radiative forcings. Some have argued that the explanation is associated with deficient parameterizations of thermally relevant processes that redistribute heat among the various climate energy reservoirs, such as those governing the rates at which heat is sequestered into the oceans [*Goddard*, 2014; *Balmaseda et al.*, 2013; *Kosaka and Xie*, 2013; *Trenberth and Fasullo*, 2013]. Another body of recent literature indicates that the discrepancies arise from a combination of uncertainties in the external forcing and model response—namely, the simulated states of the tropical Pacific may be out of phase with

observations and the internal variability of the climate system [*Santer et al.*, 2014; *Schmidt et al.*, 2014a; *Fyfe and Gillett*, 2014; *Palmer and McNeall*, 2014]. Assessing the performance of GCMs, particularly on timescales of decades or more, therefore continues to be a task of major importance [*Jansen et al.*, 2007; *Randall et al.*, 2007; *González-Rouco et al.*, 2009; *Braconnot et al.*, 2012].

Because meteorological records rarely exceed 100–200 years in duration, evaluating GCMs on decadal to centennial timescales must be accomplished using paleoclimatic data. Paleoclimate records are mainly indirect recorders of climate, most often representing responses within a complex biological, chemical, or physical system. Such records are available heterogeneously within the Earth system and have varying degrees of spatial and temporal uncertainties. Nevertheless, paleoclimate data during the Common Era (C.E.) provide multiple reconstructions of past conditions against which GCMs can be evaluated on decadal and centennial timescales [e.g., *Jansen et al.*, 2007; *Randall et al.*, 2007; *González-Rouco et al.*, 2009; *Schmidt et al.*, 2014b, 2013; *Phipps et al.*, 2013; *Fernández-Donado et al.*, 2013; *Coats et al.*, 2013].

Among the collection of paleoclimatic proxies that span the C.E., geothermal data from terrestrial borehole temperature profiles (BTPs) provide a unique estimate of past changes in the Earth's surface energy balance. Interpretations of ground surface temperature (GST) reconstructions from geothermal data often assume that long-term surface air temperature (SAT) changes are coupled to long-term GST changes. Inversion of BTPs also apply the assumption that the long-term variability of the surface energy balance propagate by thermal conduction into the subsurface where these transients are recorded as temperature anomalies with respect to the quasi steady state geothermal field.

Subsurface temperature anomalies can also be used to estimate past energy fluxes at the land surface, as well as the magnitude and rate of change of the energy stored in the continental subsurface. These latter reconstructions are less dependent on assumptions about the coupling of SATs and GSTs, an issue that has been discussed extensively in the literature [e.g., *Beltrami*, 1996; *Schmidt et al.*, 2001; *Beltrami and Kellman*, 2003; *Stieglitz et al.*, 2003; *Bartlett et al.*, 2004, 2005; *Smerdon et al.*, 2003, 2004, 2006, 2009; *Demetrescu et al.*, 2007]. In other words, the magnitude of the subsurface heat storage Q_s is independent of any surface temperature relation between SATs and GSTs. Estimating Q_s does not require the assumption of a surface temperature model or the introduction of a priori information to solve an ill-posed problem as it is the case for GST histories, but instead, Q_s is determined from direct measurement of the temperature changes at depth in response to the integrated energy balance at the ground surface. BTPs have already been used to estimate continental heat storage over the last half of the twentieth century and have shown that the continental subsurface was second only to the oceans in terms of the total amount of heat absorbed [*Beltrami*, 2002b; *Beltrami et al.*, 2002]. This continental energy calculation has thus been an important component in estimating the overall energy changes in the climate system [*Levitus et al.*, 2005; *Bindoff et al.*, 2007; *Davin et al.*, 2007; *Murphy et al.*, 2009; *Church et al.*, 2011; *Levitus et al.*, 2012; *Rhein et al.*, 2013].

As with all other climate reconstruction methods, climatic inferences from borehole geothermal data have several limitations. For instance, the spatial distribution of data is unevenly distributed across locations of opportunity. Other uncertainties relate to the complex relationship between SAT and GST at various timescales. Coupling between SAT and GST can be altered over multiple timescales by surface conditions such as snow cover trends, land use change and long-term soil moisture changes [*Baker and Ruschy*, 1993; *Pollack et al.*, 2005; *Smerdon et al.*, 2003, 2004, *Hu and Feng*, 2005; *Smerdon et al.*, 2006, 2009; *Sushama et al.*, 2006, 2007]. However, *González-Rouco et al.* [2009] have used a GCM simulation of the last millennium to show that the spatial sampling in the current International Heat Flow Commission borehole temperature database is sufficient to represent a robust global GST reconstruction and that within this simulation period SAT and GST exhibit robust long-term coupling. Additionally, studies estimating the subsurface heat storage in the later half of the twentieth century from borehole temperature data [*Beltrami*, 2002a, 2002b; *Beltrami et al.*, 2006] and indirect estimates of subsurface heat storage from meteorological records [*Huang*, 2006] yield very similar magnitudes for Q_s, implying that the ground and the lower atmosphere are thermodynamically coupled at least during this time period.

One recognized uncertainty in the interpretations of BTPs that has not been explored in terms of the impact on derived GST reconstructions at large spatial scales is the degree to which these reconstructions are affected by the maximum depth of the BTP. Because BTP data are acquired from boreholes of opportunity, the maximum measurement depth varies from 100 m to more than 1 km. The importance of the borehole depth stems from the fact that the downwelling climatic signal must be separated from the quasi steady state thermal field

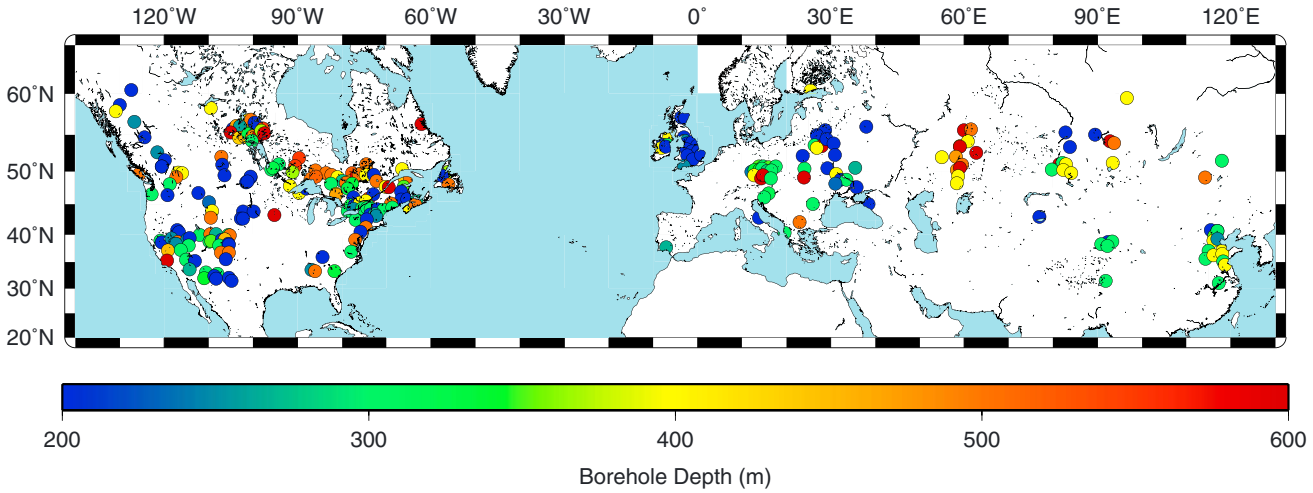

Figure 1. Dots and their colors indicate the site locations and depths, respectively, of the borehole temperature-depth profiles used in this analysis. Sites are unevenly distributed because measurements are conducted in holes of opportunity.

associated with the heat from the Earth's interior. This latter component of the signal is estimated from the lower section of a BTP, which is assumed to be unperturbed by the downwelling component of the surface signal. The validity of this assumption is dependent on the thermophysical properties of the subsurface and the character of the downwelling climatic signal, giving rise to multiple sources of uncertainty. Such uncertainties can significantly influence the magnitude of the temperature anomaly interpreted as a climatically induced signal. Until recently, there was no conclusive quantitative assessments of borehole depth impact on climate reconstructions derived from terrestrial borehole data. *Beltrami et al.* [2011] quantitatively illustrated the effects and uncertainties that arise from the analysis of a synthetic BTP truncated at different depths thus demonstrating that different GST histories can be derived from BTPs of different depths, even when the BTPs are generated under the identical surface and subsurface conditions.

In the present study, we perform a systematic analysis of terrestrial boreholes in the Northern Hemisphere (NH) as a function of borehole depth. We derive spatial GST reconstructions and estimate subsurface energy changes across available data in the NH based on BTP inversions using singular value decomposition (SVD) [e.g., *Wiggins*, 1972; *Lanczos*, 1961; *Beltrami and Mareschal*, 1991; *Mareschal and Beltrami*, 1992; *Clauser and Mareschal*, 1995; *Beltrami et al.*, 1997]. Our results represent an important real-world assessment of the degree to which borehole depths may influence temperature and energy reconstructions from borehole data and provide important empirical guidelines for depth requirements in future borehole paleoclimatic studies.

2. Theoretical Considerations

Calculations of past ground surface temperature variations from geothermal data are based on the assumption that the changes in energy imbalance at the ground surface propagate by conduction into the subsurface. Such surface energy fluctuations are recorded as perturbations of the quasi steady state thermal regime of the subsurface. That is, the subsurface thermal regime is assumed to be in a long-term equilibrium resulting from the balance of the energy contributions from the interior of the Earth and the long-term climatic conditions at the surface. As the contribution from the interior of the Earth is constant on the scale of millions of years, any perturbation in the shallow subsurface is interpreted as a record of recent changes in climate at the ground surface. Because of the nature of heat diffusion, seasonal fluctuations typically do not penetrate more than 15 m, centennial-scale surface changes are recorded in the upper 120 m, and millennial-scale GST changes are preferentially recorded in the upper 500 m of the subsurface although all contributions are integrated as subsurface heat content in the subsurface [*Bodri and Cermak*, 2007]. Thus, the analysis of the subsurface temperature perturbation, $T_t(z)$, as a function of depth from measurements in a borehole allows an estimate of the energy balance history at the ground surface.

In this framework, the temperature at depth z, $T(z)$, is then given by [*Carslaw and Jaeger*, 1959]:

$$T(z) = T_0 + q_0 R(z) + T_t(z) \quad (1)$$

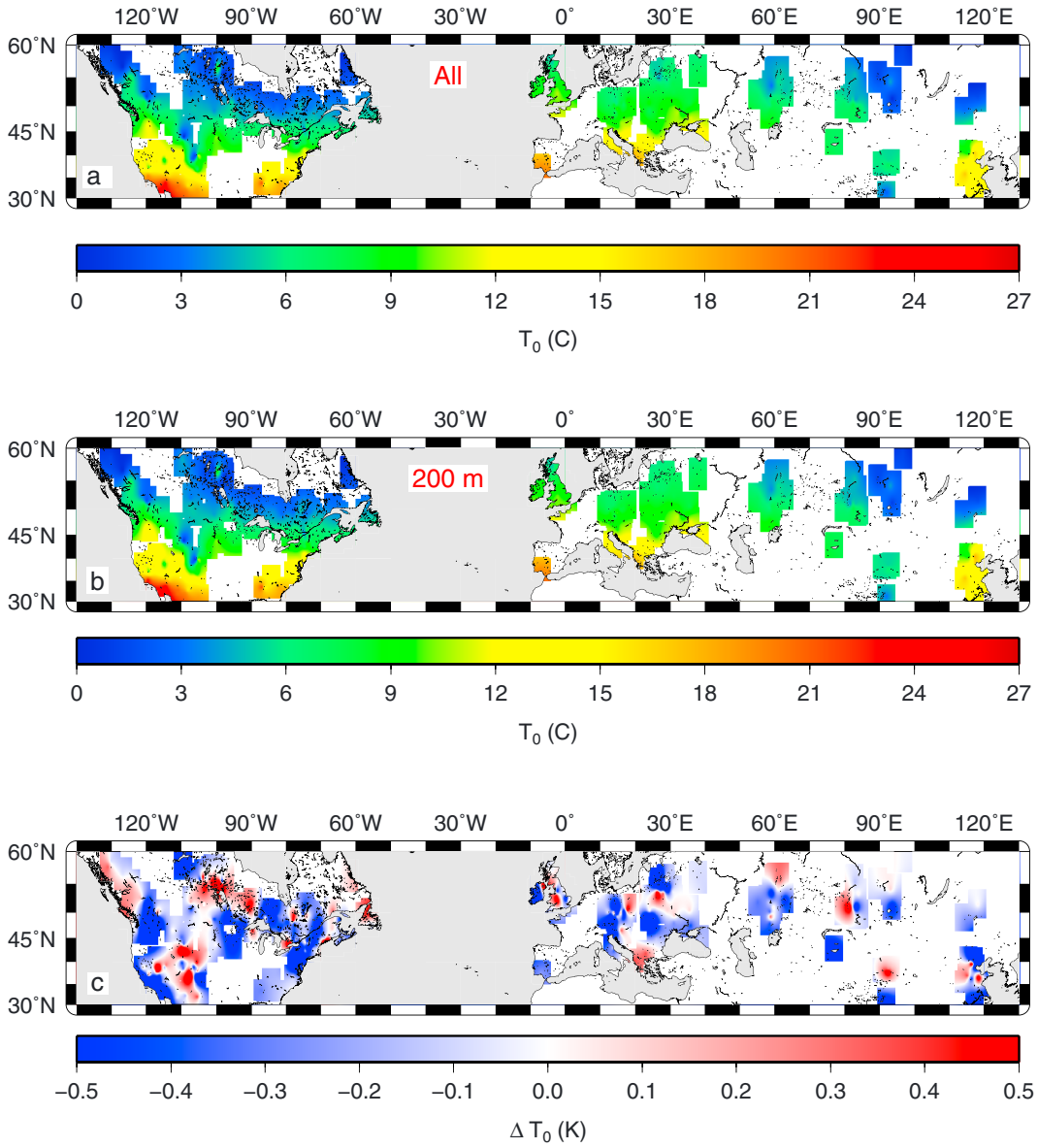

Figure 2. Spatial distribution of the long-term surface temperature estimated from the semiequilibrium steady state temperature versus depth profiles. (a) T_0 spatial distribution for all profiles without depth selection, (b) T_0 spatial distribution from the analysis of temperature profiles truncated at 200 m, (c) ΔT_0 spatial distribution for the difference between Figure 2a and Figure 2b. This represents a potential uncertainty in the determination of T_0 as a function of depth [*Beltrami et al.*, 2011].

where T_0 is a long-term temperature reference at the ground surface, q_0 is the surface heat flow density, and $R(z)$ is the thermal depth. In other words $T_0 + q_0R(z)$ is the quasi steady state geothermal profile from which subsurface temperature anomalies, $T(t)(z)$, are estimated [e.g., *Lewis*, 1992; *Bodri and Cermak*, 2007].

For a given borehole temperature versus depth profile, the set of n temperature-depth data forms a system of n linear equations. Together with the assumption of a model consisting of a series of k surface temperature step variations in time, these n linear equations form a system of linear equations with k unknowns that can be inverted to obtain a series of ground surface temperature estimates, representing the GST histories at the site. The inversion used here is singular value decomposition (SVD) [e.g., *Mareschal and Beltrami*, 1992; *Clauser and Mareschal*, 1995; *Beltrami et al.*, 1997]. The spatial analysis performed in this work follows the same procedure as in *Beltrami and Bourlon* [2004] for consistency.

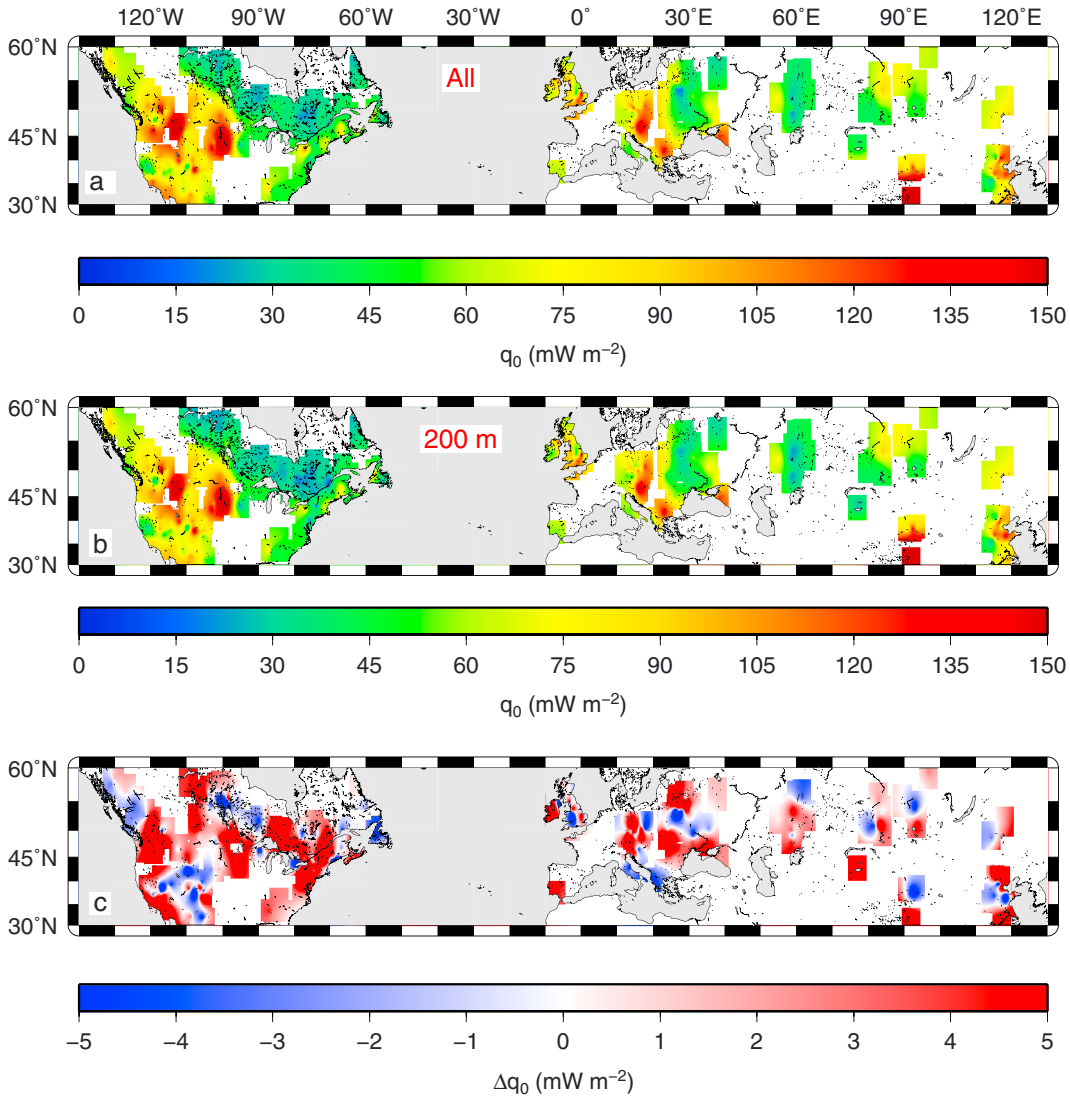

Figure 3. Spatial distribution of the semiequilibrium heat flow density from the interior of the Earth, i.e., the long-term lower boundary condition. (a) q_0 spatial distribution for the complete temperature profile data set, (b) q_0 spatial distribution for temperature profiles truncated at 200 m, and (c) Δq_0 spatial distribution for the difference between Figure 3a and Figure 3b. This represents a potential uncertainty in the determination of q_0 as a function of depth [*Beltrami et al.*, 2011].

Unlike the inversion procedure that requires the assumption of a model as well as a priori information, the estimate of the subsurface heat content is more robust as it can be determined by minimal assumptions. Changes in the energy balance (imbalance) at the Earth's surface propagate and are recorded as temperature anomalies as described above; these can also be interpreted as superimposing changes in energy accumulation in the subsurface. To estimate the change in subsurface energy Q_s, no surface model assumption is needed and only the BTP and the thermal properties are required. The subsurface heat content can be written as follows:

$$Q_s = \rho c \int_{z_{\min}}^{z_{\max}} T_t(z)\mathrm{d}z, \tag{2}$$

where ρc is the volumetric heat capacity, $z_{\min}$ and $z_{\max}$ represent the integration depth range, and T_t is the temperature perturbation as a function of depth. That is, the subsurface heat content is proportional to the area under the curve defined by the estimated subsurface temperature anomaly profile. This characteristic

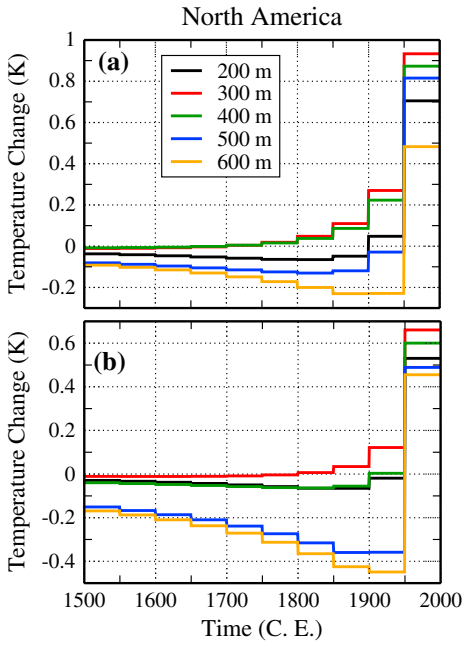

Figure 4. Mean ground surface temperature histories for North America estimated for temperature profiles of varying depths as indicated in legend. (a) All boreholes in North America; (b) subset of 35 deep boreholes GST histories to eliminate the masking effect of the spatial variability and depth-related data depopulation of the larger data set.

therefore makes the estimate of Q_s dependent on the depth of the subsurface temperature anomaly range, the choice of fitting range for the determination of the quasi steady state geothermal regime and thus the depth of the BTP.

3. Methods and Data

For consistency with *Beltrami and Bourlon* [2004] and *Beltrami et al.* [2006], the GST model for each individual SVD inversion is a series of 10 time steps of 50 year duration. The value of thermal diffusivity is set at 10^{-6} m^2 s^{-1}. The choice of thermal diffusivity and its impact on the subsurface anomalies have been previously explored [e.g., see *Beltrami et al.*, 2011, Figure 3]. Thermal diffusivity also affects the model time span used for GST histories reconstructions; however, data for the thermal properties of the subsurface are not available for the great majority of the sites in the International Heat Flow Commission (IHFC) database. Thus, a requirement for data inclusion in the IHFC database is that if lithological changes are systematic for a data set, corrections must be applied using data from thermal properties as a condition for inclusion in the database. If there are no systematic variations in the lithology as determined from each borehole's lithological log, then a constant value of the thermal properties is used. After such corrections, it is customary in the borehole climatology literature to use a value of 10^{-6} m^2 s^{-1} for the thermal diffusivity, κ, which depends on the ratio of the volumetric heat capacity, ρC, and thermal conductivity, λ ($\kappa = \frac{\lambda}{\rho C}$) of the materials in the subsurface. λ and ρC can change in the subsurface and over a wide range, but they do so in compensating directions yielding a relatively narrow range ($\pm$10%) of values for their ratio, i.e., the thermal diffusivity. Thus, for a subsurface temperature log exhibiting high-frequency variability of the thermal properties about a mean value, the assumption of constant thermal diffusivity properties is reasonable.

For the SVD inversions, the singular value cutoff was set to 0.3, keeping five principal components for all of the temperature-depth profiles included in the reconstruction. This choice of the same eigenvalue cutoff, retained number of principal components, and sampling rate, i.e., the same problem geometry, for each BTP data, ensures that the resolution of the individual inversions is the same, allowing spatial analysis to be performed.

Each SVD inversion yields the long-term surface temperature T_0, semiequilibrium steady state geothermal heat flow density q_0, and the recent transient surface temperature changes T_t from the data. These GST changes are expressed throughout this paper as departures from the long-term mean T_0. The geothermal reconstructions of recent past surface temperatures assume that there is no significant climate variation on scales longer than 500 years. We note here that the time of data acquisition, which is taken into account in the inversion for the determination of GST histories, also adds to the sources of uncertainties, but it is not a part of the analyses of the present work. BTPs for 611 sites in the NH are used for our analysis. Three hundred seventy-two of these sites are located in North America, 120 sites are in Europe, and 119 sites are in Asia. Most of the data for these sites were obtained and selected from the IHFC database, available at the National Climate Data Center for Paleoclimatology (NOAA). We point out, however, that not all data listed in the database are available. Data from India [*Roy et al.*, 2002] and Russia [*Pollack et al.*, 2003] remain inaccessible to the scientific community. The rest of the database was obtained from the BTP database for Canada at Center for Research in Isotopic Geochemistry and Geochronology, Université du Québec á Montréal.

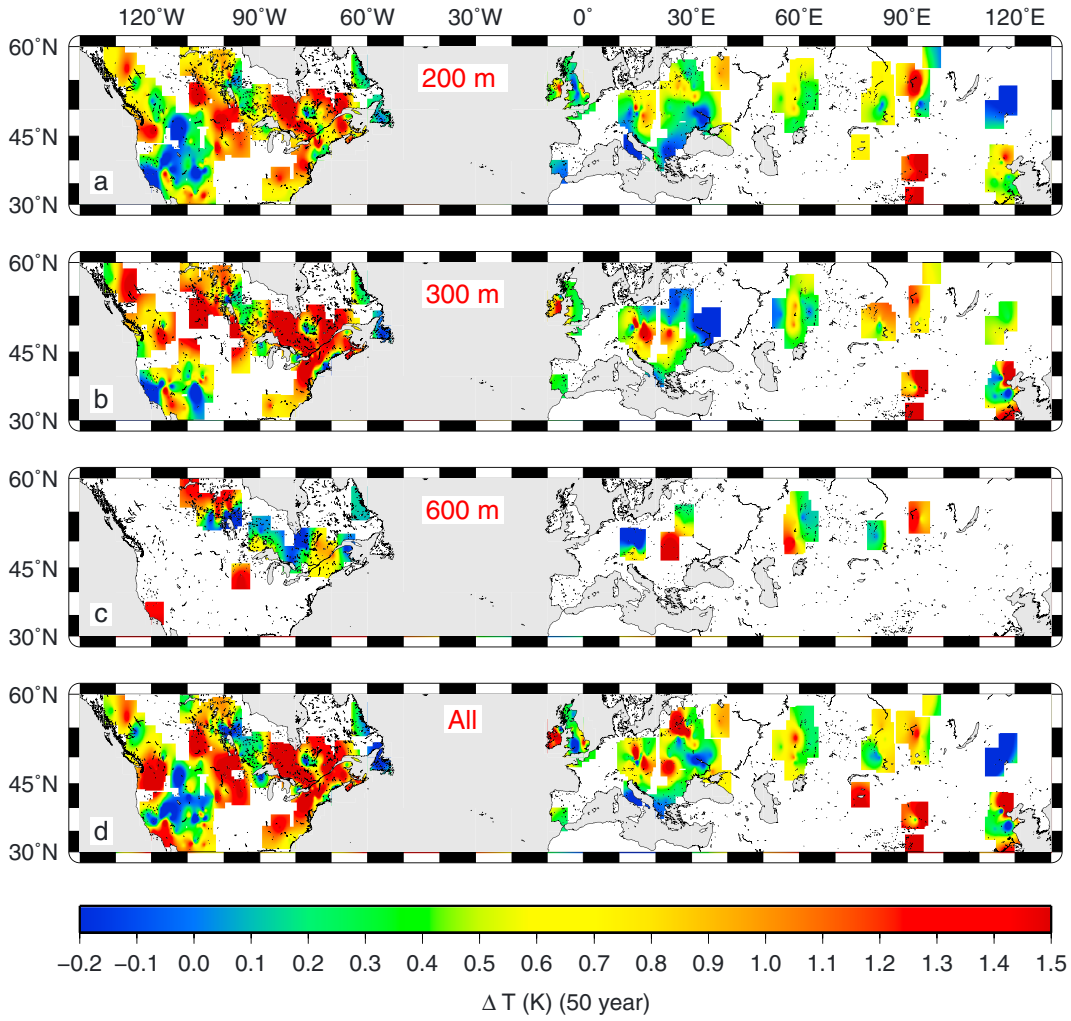

Figure 5. Spatial distribution of the ground surface temperature history for the most recent 50 years before present using progressively deeper depths of borehole truncations. Spatial distribution for temperature profiles truncated at (a) 200 m, (b) 300 m, (c) 600 m and, (d) all profiles without depth selection. The figure is constructed from inversion of 611 temperature-depth profiles in the Northern Hemisphere between 30°N and 60°N. All inversions included in the analysis are performed with the same eigenvalue cutoff. The same number of principal components were included in the reconstruction of each GST history.

The spatial distribution of the data set is shown in Figure 1. (For details on the gridding procedure see *Beltrami and Bourlon* [2004].)

4. Results and Discussion

4.1. Semiequilibrium Geothermics: Depth Dependence

Determining the semiequilibrium surface temperature T_0 from a BTP has been shown to be depth dependent [e.g., see *Beltrami et al.*, 2011, Figures 4 and 10]. In all large-scale analyses to date, however, the effects of differences in BTP depths on the results have remained unquantified. Recall that due to the rate of propagation of the surface energy imbalances and because the timing of the propagation of energy perturbations at the surface are related to the square of the depth (i.e., $t \propto z^2$) [*Carslaw and Jaeger*, 1959], BTPs of different depths reflect the energy imbalance history at the surface over a different time period, assuming that the thermal properties are the same. That is, given two BTPs of different depths subjected to the same history of energy imbalance at the surface, two different long-term surface temperatures T_0 would be retrieved, indicating different states of semiequilibrium or initial conditions. Thus, a joint analysis of such two BTPs would yield results that would not reproduce the exact same GST history because the reference against which each analysis is performed would be different. This in turn would affect the timing of the resolved events and their

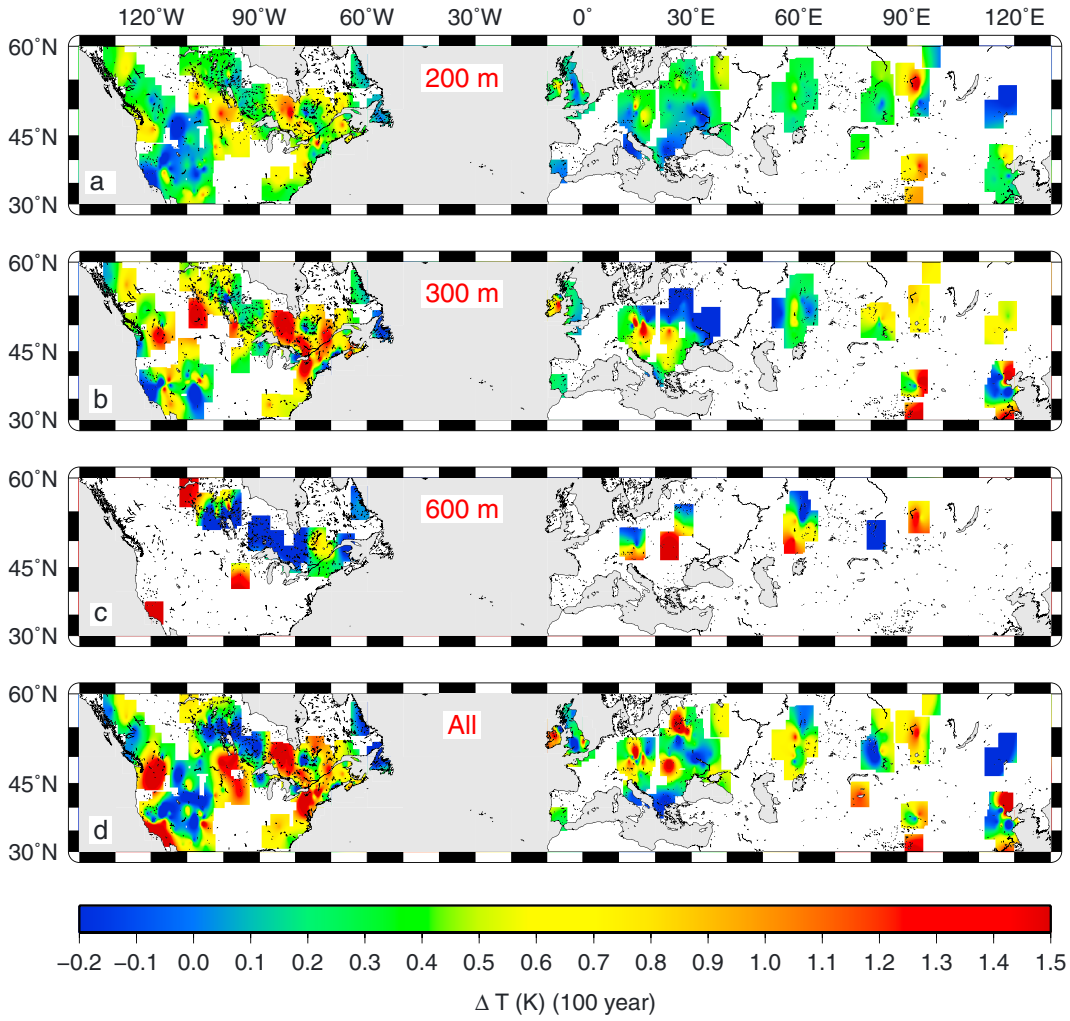

Figure 6. Spatial distribution of the ground surface temperature history for the most recent 100 years before present using progressively deeper depths of borehole truncation. Spatial distribution for temperature profiles truncated at (a) 200 m, (b) 300 m, (c) 600 m and, (d) all profiles without depth selection. The figure is constructed from inversion of 611 temperature-depth profiles in the Northern Hemisphere between 30°N and 60°N. All inversions included in the analysis are performed with the same eigenvalue cutoff. The same number of principal components were included in the reconstruction of each GST history.

magnitudes in a unique manner dependent on their specific depth differences, the climate-induced surface energy imbalance history at the surface, and the subsurface thermal properties. The exception to the above is the case in which the depth differences occur below the penetration depth of the recent surface energy imbalances.

4.2. Determining T_0 and q_0

Figure 2 shows the spatial distribution of the semiequilibrium surface temperature T_0 for the complete data set in Figure 1. In Figure 2a, T_0 is determined from the analysis of all BTPs regardless of their depths. That is, T_0 is determined from the extrapolation to the surface of the least squares fit to the bottom most 100 m of each profile without regard to their depths. There are special cases where BTPs exhibit large recent records of climate change where the method of *Roy et al.* [2002] can be used to estimate the local minimum of variation for the geothermal gradient and thus better constrain the quasi steady state profile. For cases in which spatial analyses are performed that rely on deep BTP or BTPs recording a variety of climatic histories, such method cannot be applied. Figure 2b shows the estimate of T_0, but for the case in which all BTPs have been truncated at 200 m. Both sets of surface temperatures show a steady increase with decreasing latitudes as expected. Figure 2c maps the difference between Figures 2a and 2b and thus represents the potential uncertainty associated with estimates of T_0 from BTPs of different depths. Differences are in the range of 1 K (± 0.5°K), which

are less than 4% if the data for T_0 in the spatial distribution map is considered at face value. This temperature difference is, however, on the same order of magnitude as surface temperature changes during the twentieth century and therefore represents a potentially significant source of uncertainty.

Similar to Figure 2, Figure 3a displays the estimates of q_0 from the complete data set of BTPs, regardless of depth, and Figure 3b shows q_0 estimated from all BTPs truncated at 200 m. Heat flow density, $q = -\lambda \frac{dT(z)}{dz}$, as a function of depth was estimated from the linear fit described above and from the semiequilibrium gradient ($\Gamma = \frac{dT(z)}{dz}$, assuming a homogeneous subsurface with constant thermal conductivity $\lambda = 3.0$ W K^{-1} m^{-1}). The differences are in the range of 10 mW/m^2 which correspond to uncertainties in q_0 as high as 20% of the typical values of heat flow density found in the literature at some of these locations [*Jaupart and Marechal*, 2011].

4.3. GST Histories as a Function of Depth

Determining GST histories from BTPs involves solving an imperfect problem with nonunique solutions. Selecting the optimal solution requires a priori information and other assumptions determining the character of the model being evaluated. These analyses have been customary in borehole climatology [*Huang et al.*, 2000a; *Harris and Chapman*, 2001; *Beltrami and Bourlon*, 2004]. Here we carry out individual inversions for each BTP used in the previously cited works assuming the same GST model and identical eigenvalue cutoff for the data set with well-defined depth ranges. We then obtain the mean GST history for a variety of chosen truncation depths. The resulting mean GST histories are shown in Figure 4a. These results are consistent with those of *Beltrami et al.* [2011] and indicate that differences in maximum borehole depths introduce uncertainties in the magnitude and shape of the subsurface temperature anomaly. These biases consequently influence the estimated magnitude and temporal characteristics of recovered mean GST histories. Results in Figure 4a imply that the comparison of reconstructed GST histories from temperature profiles with different maximum depths should be done with caution as they do not contain the same proportion of climatic information from the change in upper boundary condition over the same time interval [see, for example, *Vasseur et al.*, 1983], and the magnitudes of reconstructed temperatures at the surface are not referenced to the same initial conditions. Note that the number of deep BTPs is small; thus, the number of BTPs available for analysis decreases rapidly with increasing maximum depth requirements (i.e., 372 and 35 BTPs at 200 and 600 m, respectively). Thus, an important caveat of these and subsequent results that show depth dependencies is that the results are influenced by sampling differences in the number of boreholes that are available to the specified depth ranges. Figure 4b illustrates a similar analysis as shown in Figure 4a, but for a subset of 35 deep (600 m) borehole temperature profiles in a small region of Canada (see Figure 1 for site locations). Results are similar of those in Figure 4a; however, the resulting GST histories are not representative of North America and are not comparable to the case in Figure 4a. The climate variability recorded in these BTPs is specific to this region, which was subject to a cooling period between approximately 1600 and 1800 C.E. associated with the Little Ice Age in North America [*Beltrami et al.*, 1992]. The largest component of the signal for this large event is recorded below a depth of 200 m; thus, the depth dependency effect appears much more accentuated than the hemispheric means in Figure 4a.

4.3.1. Spatial Distribution of GST as a Function of Depth

Figures 5a–5c and 6a–6c show the respective spatial distribution of the mean GST change between 1950 and 2000 C.E. (i.e., the first model step at 50 a B.P.) and 1900 to 2000 C.E. (i.e., the first two model steps at 100 a B.P.), based on inversions of the BTPs available to the indicated depths listed in the figures. The spatial distribution of the 1950–2000 temperature change does not significantly differ for the depth ranges of 200 and 300 m other than showing differences due to the depletion of data, as compared with the results from analyses for which all data, regardless of BTP depth, were included (Figure 5d). These results are consistent because the most recent temperature step change would be recorded within the upper 80 m of the subsurface. On the other hand, large differences appear for the spatial distribution for the same time interval in the case of the 600 m depth range. This is expected because deeper BTPs contain remnants of previous climate events that have left their energy contributions distributed over a wide depth range in the subsurface. The spatial averaging in Figure 5c is also altered because of grid cell population change.

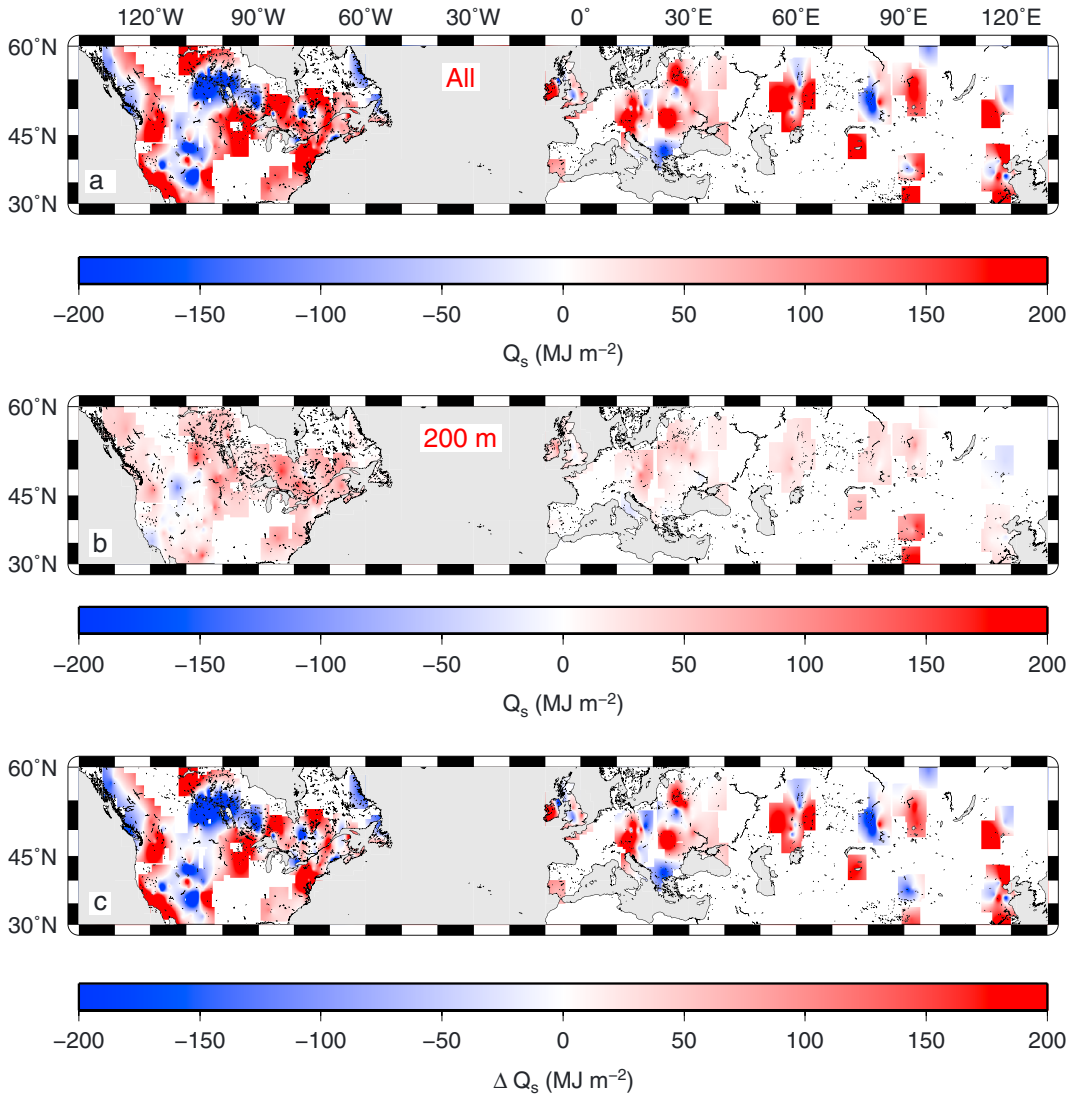

Figure 7. Spatial distribution of the cumulative heat stored in the subsurface Q_s (MJ m^{-2}) as estimated from (a) the complete temperature profile data set, (b) from the set of temperature profiles truncated at 200 m, and (c) spatial distribution of ΔQ_s for the difference between Figure 7a and Figure 7b.

Figure 6a shows the 1900–2000 temperature change for an analysis of BTPs in the range of 200 m. The differences here, unlike in the 1950–2000 case, are larger because the detectable thermal signal over the last 100 years would be expected to reach depths of about 150 m. When considering 200 m deep BTPs, the lower most 100 m of the BTP is used to determine the reference temperature T_0, and thus, some of the perturbation associated with the last 100 year period is lost in this procedure. However, BTPs to a depth of 300 m, shown in Figure 6b, retain most of the 100 year changes, and therefore, the differences between Figures 6b and 6d are smaller. Again, larger differences appear in the spatial distribution for the case of the 600 m depth range for the same reasons as discussed above for the results in Figure 5.

Table 1. Mean Subsurface Heat Content for Canada for Various Depth Ranges[a]

Depth Range (m)	Q_s (× 10^{21} J)
0–200	0.3157
0–300	0.5829
0–400	0.2542
0–500	−1.3502
0–600	−1.9752

[a]Estimates are an extrapolation from only 35 available borehole temperature-depth profiles over a relatively small region in Central and Eastern Canada.

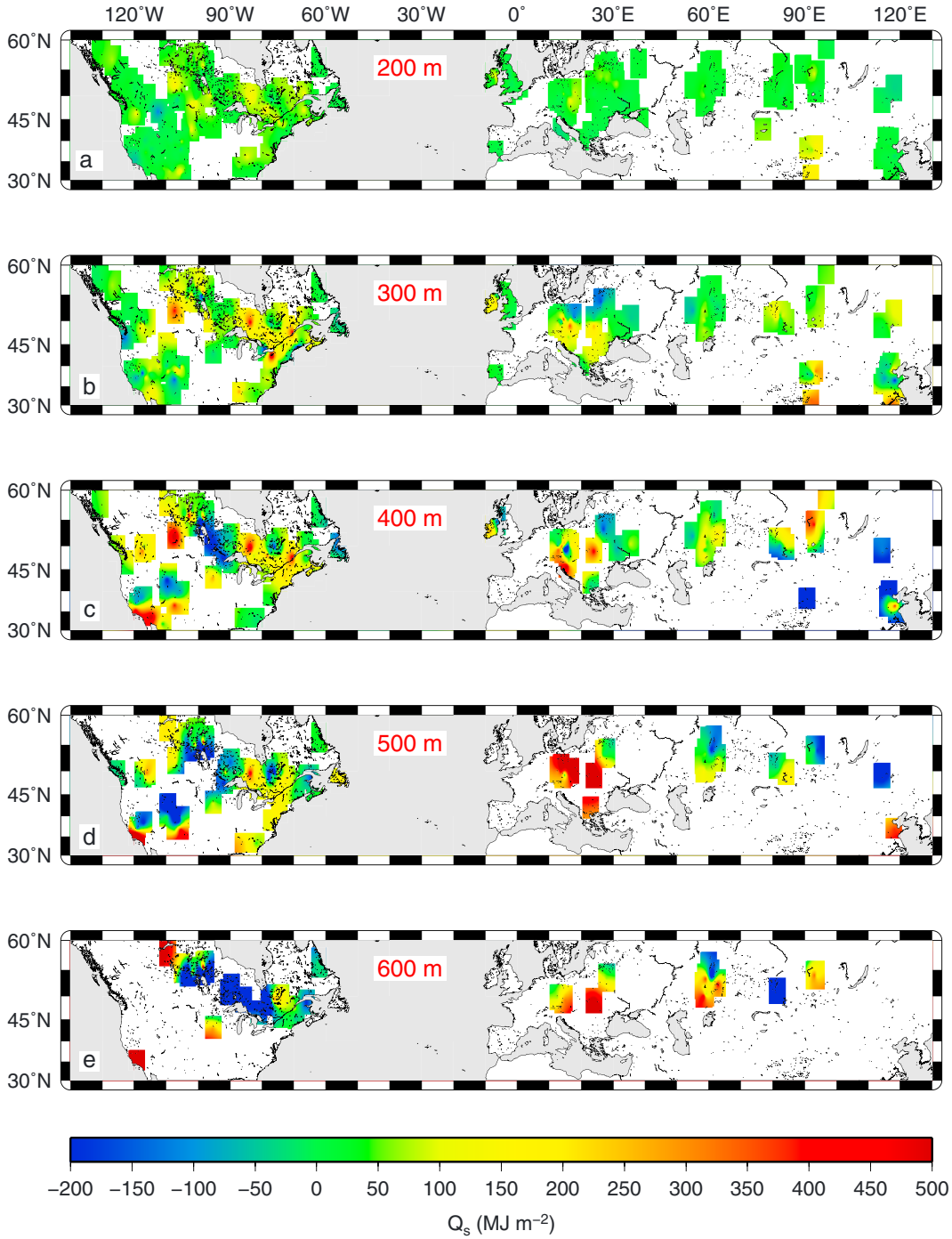

Figure 8. Spatial distribution of total terrestrial heat gain, Q_s (MJ m^{-2}), as a function of the maximum BTP depth in the Northern Hemisphere between 30°N and 60°N. Spatial distribution for temperature profiles truncated at (a) 200 m, (b) 300 m, (c) 400 m, (d) 500 m, and (e) 600 m.

4.4. Continental Heat

We also examine the dependency of continental heat storage estimates on the maximum depth of the BTPs. The subsurface thermal anomalies are proportional to the total heat absorbed or released by the ground, such that the integral of the temperature anomalies versus depth is directly proportional to the heat stored in the subsurface as described in equation (2). Figure 7 shows the spatial distribution of subsurface heat defined in equation (2) for an assumed constant value of volumetric heat capacity, ρc, set at 3×10^6 J m^{-3} K^{-1} after

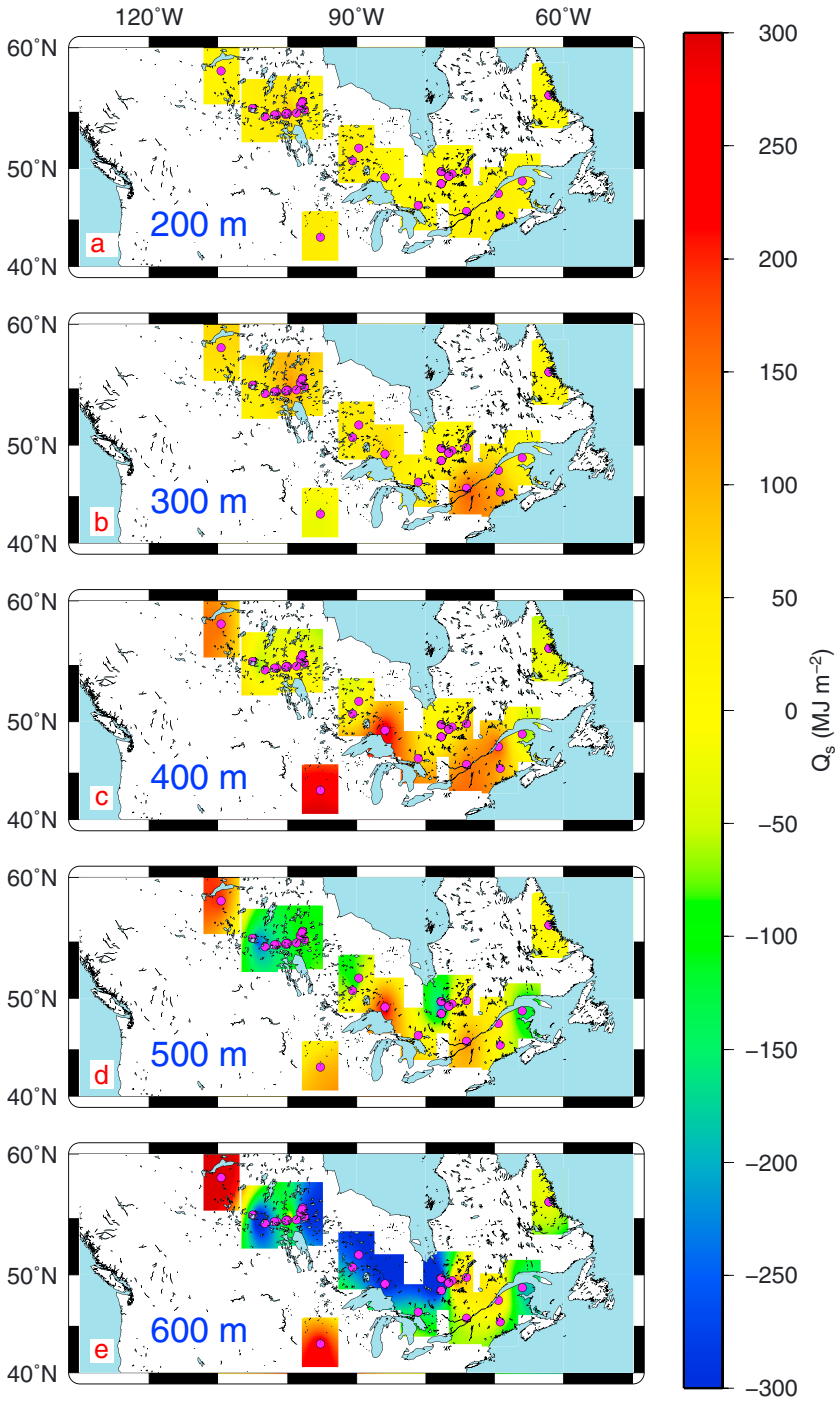

Figure 9. Spatial distribution of total terrestrial heat gain, Q_s (MJ m^{-2}), as a function of maximum BTP depth for the 35 profiles reaching a depth of 600 m in Canada. Most of this area of Canada was affected by a cold period during the Little Ice Age interval. Spatial distribution for temperature profiles truncated at (a) 200 m, (b) 300 m, (c) 400 m, (d) 500 m, and (e) 600 m.

Čermák and Rybach [1982]. Figure 7a shows the spatial distribution of the subsurface heat content, Q_s, estimated from the complete BTP database with the full range of depths. Figure 7b shows Q_s, but for the case where all BTPs have been truncated at 200 m. For this case there is less spatial variability in subsurface energy than for the case of the full data set, which can be considered evidence of a recent generalized energy increase in the region's subsurface. The differences between Figure 7a and Figure 7b are large as illustrated in Figure 7c,

because the integral defining Q_s spans the entire subsurface temperature anomaly depth range; Q_s is therefore expected to be different as greater depths include a larger temperature anomaly and thus include the thermal response of the ground to older events. Some of these older events have contributed negative subsurface anomalies (i.e., colder events; see Table 1) as is the case for most areas of Canada and northern Europe where the existence of the Little Ice Age (LIA) has been documented from boreholes ranging from 400 to 600 m in depth [e.g., *Beltrami et al.*, 1992; *Lewis*, 1992; *Luterbacher et al.*, 2006]. These subsurface heat content differences are expected to also vary spatially and with depth depending on the previous specific climatic history at the surface for each BTP site, e.g., the areas affected by the last glacial cycle in high northern latitudes [e.g., *Rath et al.*, 2012; *Beltrami et al.*, 2014].

Figure 8 shows the details of the spatial distribution of changes in subsurface heat content for a range of depths of BTP truncation. The signals of the LIA are clearly visible in Central and Eastern Canada [*Shen and Beck*, 1992; *Beltrami et al.*, 1992; *Beltrami and Mareschal*, 1992; *Beltrami et al.*, 1997, 2011]. Some sites show positive heat gains with increasing depth in parts of Europe; some of this warming signal at depth could be the result of land use changes that started several centuries in the past [*Nitoiu and Beltrami*, 2005; *Ferguson and Beltrami*, 2006].

In order to eliminate the effects of decreasing spatial sampling as the maximum borehole depth truncation is increased, we estimated Q_s from only the subset of 35 BTPs reaching 600 m (see Table 1). Although these sites in Figure 9 are all located in Central and Eastern Canada and are not to be taken as representative of all of Canada, they provide an opportunity to *illustrate* the effects of past events on the subsurface energy balance and show that the energy gain is restricted to the shallow subsurface or temporally recent events. The numerical values for subsurface heat have been extrapolated to the area of Canada assuming an area of 9.985×10^{12} m^2 (Table 1).

5. Conclusions

5.1. Implications for GST Histories

The maximum depth of BTPs used in borehole climatology has been shown, in a synthetic experiment, to have an impact on the determination of the initial conditions, on the calculated subsurface climatic signal, and therefore on the results of GST inversion [*Beltrami et al.*, 2011]. Here we have performed an analysis for the complete data set of the Northern Hemisphere taking into account depth differences and comparing them with previous analyses of the unfiltered data set. We confirm that the origin of the uncertainties due to the maximum depth of BTPs arise because downward propagation of past surface temperature changes (> 1000 years before present (B.P.)) continue to have a nonnegligible contribution to the thermal state of the subsurface at the depth range where the determination of the equilibrium surface temperature, T_0, and geothermal gradient, Γ_0, are carried out [*Rath et al.*, 2012; *Beltrami et al.*, 2014]. This quasi steady state acts as the reference and initial conditions that allows retrieval of the historically driven energy balance changes at the surface. For the comparisons between the spatial analysis of the complete data set and one limited by a common depth of 200 m, our results show that uncertainties in the estimates of the long-term surface temperature, extrapolated from the quasi steady geothermal gradient, are in the range of $\pm$0.5 K for the complete Northern Hemisphere data set. The variability at individual sites is generally much smaller. Similarly, the uncertainties in the estimates of the heat flow density, inferred from the quasi steady state geothermal gradient, are $\pm$5 mW m^{-2}. Since previous global analyses required BTPs to a minimum depth of 200 m or deeper [*Huang et al.*, 2000b; *Harris and Chapman*, 2001; *Beltrami*, 2002b; *Beltrami and Bourlon*, 2004; *Pollack and Smerdon*, 2004], our ensemble spatial results show that recent GST changes are robust for 200 m deep BTPs, as compared to results from the unfiltered database. However, GST histories estimated for time periods further back into the past with the unfiltered data set should be revised to take into account the depth of the BTPs. As discussed above, this effect is clearly visible in Figure 6, where the choice of BTP depth, and the spatial distribution of the temperature change for the time interval in question (1900–2000) is significantly different from the unfiltered database results.

We demonstrate above that the effect of borehole depth on the spatial distribution of the ground temperature estimates from subsurface temperatures becomes visible even for the most recent 100 year interval. Future GST history spatial analysis should be done using only borehole temperature profiles of the same thermal depth; that is, ground temperature history models should be evaluated for data sets that cover the

same depth range (i.e., recording the same temporal extent of climatic variations at the surface) and have the same initial conditions, such that the subsurface temperature anomalies as a function of depth are comparable. Individual inversions can be done for any borehole depth, but such results should only be compared with inferences from other boreholes when the depth ranges analyzed are the same. Where this is not done, discrepancies induced by depth difference could be significant, as illustrated in Figure 7c.

5.2. Implications for Subsurface Heat Content

For the comparison between the spatial analysis of the complete data set and that limited to a common depth of 200 m, the spatial distribution of the subsurface heat content shows considerable variability. Some of this variability arises because the IHFC database comprises borehole temperature logs acquired since the late 1960s spanning a 40 year period; thus, there is a component of the variability on Q_s arising from the differences in dates of measurement. Additionally, because Q_s is proportional to the magnitude of the depth of the subsurface temperature anomaly, borehole depth differences are also a source of variability. Furthermore, deep boreholes may contain signals of previous major climatic events such as the last glacial cycle, while such signals are not detectable in shallow boreholes [*Beltrami et al.*, 2014].

The uncertainties described above explain the differences between a corrected and an uncorrected analysis. However, our new corrected estimates of the subsurface heat content spatial distribution, Q_s, for a common depth of 200 m provide important information for use in land surface model schemes, i.e., initial conditions (T_0), bottom boundary conditions (q_0), and an independent estimate of subsurface energy content Q_s. Our corrected results therefore should be collectively useful for assessments of energy exchanges between the atmosphere and the ground by land surface components of GCMs and regional climate models for century-scale simulations, in particular those with deep bottom boundaries in their land surface components that include comprehensive aboveground and belowground thermodynamical processes.

Acknowledgments

This work was supported by grants from the Natural Sciences and Engineering Research Council of Canada Discovery Grant (NSERC DG 140576948) program and the Atlantic Innovation Fund (AIF-ACOA) to H. Beltrami. We are grateful to Atlantic Computational Excellence Network (ACEnet) for computational resources. Lamont-Doherty Earth Observatory contribution 7897. The data for this paper are available at NOAA's National Climatic Data Center: http://www.ncdc.noaa.gov/data-access/paleoclimatology-data/datasets/borehole.

References

Baker, D. G., and D. L. Ruschy (1993), The recent warming in eastern Minnesota shown by ground temperatures, *Geophys. Res. Lett.*, *20*, 371–374.

Balmaseda, M. A., K. E. Trenberth, and E. Källén (2013), Distinctive climate signals in reanalysis of global ocean heat content, *Geophys. Res. Lett.*, *40*, 1754–1759, doi:10.1002/grl.50382.

Bartlett, M. G., D. S. Chapman, and R. N. Harris (2004), Snow and the ground temperature record of climate change, *J. Geophys. Res.*, *109*, F04008, doi:10.1029/2004JF000224.

Bartlett, M. G., D. S. Chapman, and R. N. Harris (2005), Snow effect on North American ground temperatures, 1950–2002, *J. Geophys. Res.*, *110*, F03008, doi:10.1029/2005JF000293.

Beltrami, H. (1996), Active layer distortion of annual air/soil thermal orbits, *Permafrost Periglac. Processes*, *7*, 101–110.

Beltrami, H. (2002a), Climate from borehole data: Energy fluxes and temperatures since 1500, *Geophys. Res. Lett.*, *29* (23), 2111, doi:10.1029/2002GL015702.

Beltrami, H. (2002b), Earth's long term memory, *Science*, *297*, 206–207.

Beltrami, H., and E. Bourlon (2004), Ground warming patterns in the Northern Hemisphere during the last five centuries, *Earth Planet. Sci. Lett.*, *227*, 169–177.

Beltrami, H., and L. Kellman (2003), An examination of short- and long-term air-ground temperature coupling, *Global Planet. Change*, *38*, 291–303.

Beltrami, H., and J.-C. Mareschal (1991), Recent warming in Eastern Canada inferred from geothermal measurements, *Geophys. Res. Lett.*, *18*(4), 605–608.

Beltrami, H., and J.-C. Mareschal (1992), Ground temperature histories for Central and Eastern Canada from geothermal measurements: Little Ice Age signature, *Geophys. Res. Lett.*, *19*, 689–692.

Beltrami, H., A. M. Jessop, and J.-C. Mareschal (1992), Ground temperature histories in Eastern and Central Canada from geothermal measurements: Evidence of climate change, *Palaeogeogr. Palaeoclimatol. Palaeoecol.*, *98*, 167–184.

Beltrami, H., L. Cheng, and J.-C. Mareschal (1997), Simultaneous inversion of borehole temperature data for determination of ground surface temperature history, *Geophys. J. Int.*, *129*, 311–318.

Beltrami, H., J. E. Smerdon, H. N. Pollack, and S. Huang (2002), Continental heat gain in the global climate system, *Geophys. Res. Lett.*, *29*(8), 8-1–8-3, doi:10.1029/2001GL014310.

Beltrami, H., E. Bourlon, L. Kellman, and J. F. González-Rouco (2006), Spatial patterns of ground heat gain in the Northern Hemisphere, *Geophys. Res. Lett.*, *33*, L06717, doi:10.1029/2006GL025676.

Beltrami, H., J. E. Smerdon, G. S. Matharoo, and N. Nickerson (2011), Impact of maximum borehole depths on inverted temperature histories in borehole paleoclimatology, *Clim. Past*, *7*, 745–756.

Beltrami, H., G. S. Matharoo, L. Tarasov, V. Rath, and J. E. Smerdon (2014), Numerical studies on the impact of the last glacial cycle on recent borehole temperature profiles: Implications for terrestrial energy balance, *Clim. Past*, *10*, 1693–1706.

Bindoff, N., et al. (2007), Observations: Oceanic climate change and sea level, in *Climate Change 2007: The Physical Science Basis. Contribution of Working Group I to the Fourth Assessment Report of the Intergovernmental Panel on Climate Change*, edited by S. Solomon et al., Cambridge Univ. Press, Cambridge, U. K., and New York.

Bodri, L., and V. Cermak (2007), *Borehole Climatology: A New Method How to Reconstruct Climate*, Elsevier, Oxford.

Braconnot, P., S. P. Harrison, M. Kageyama, P. J. Bartlein, V. Masson-Delmotte, A. Abe-Ouchi, B. Otto-Bliesner, and Y. Zhao (2012), Evaluation of climate models using palaeoclimatic data, *Nat. Clim. Change*, *2*, 417–424.

Carslaw, H. S., and J. C. Jaeger (1959), *Conduction of Heat in Solids*, p. 243 2nd ed., Oxford Univ. Press, London.

Čermák, V., and L. Rybach (1982), Thermal conductivity and specific heat of minerals and rocks, in *Landolt Börnstein: Physical Properties of Rocks, Group V, Geophysics*, vol. 1a, edited by G. Angenheister, pp. 305–343, Springer, Berlin.

Church, J. A., N. J. White, L. F. Konikow, C. M. Domingues, J. G. Cogley, E. Rignot, J. M. Gregory, M. R. van den Broeke, A. J. Monaghan, and I. Velicogna (2011), Revisiting the Earth's sea-level and energy budgets from 1961 to 2008, *Geophys. Res. Lett.*, *38*, L18601, doi:10.1029/2011GL048794.

Clauser, C., and J.-C. Mareschal (1995), Ground temperature history in central Europe from borehole temperature data, *Geophys. J. Int.*, *121*, 805–817.

Coats, S., E. Smerdon, R. Seager, B. Cook, and J. González-Rouco (2013), Megadroughts in Southwestern North America in millennium-length ECHO-G simulations and their comparison to proxy drought reconstructions, *J. Clim.*, *26*, 7635–7649.

Davin, E. L., N. de Noblet-Ducoudré, and P. Friedlingstein (2007), Impact of land cover change on surface climate: Relevance of the radiative forcing concept, *Geophys. Res. Lett.*, *34*, L13702, doi:10.1029/2007GL029678.

Demetrescu, C., D. Nitoiu, C. Boroneant, A. Marica, and B. Lucaschi (2007), Thermal signal propagation in soils in Romania: Conductive and non-conductive processes, *Clim. Past*, *3*, 637–645.

Ferguson, G., and H. Beltrami (2006), Transient lateral heat flow due to land-use changes, *Earth Planet. Sci. Lett.*, *252*, 217–222, doi:10.1016/j.epsl.2005.12.001.

Fernández-Donado, L., et al. (2013), Large-scale temperature response to external forcing in simulations and reconstructions of the last millennium, *Clim. Past*, *9*, 393–421.

Fyfe, J. C., and N. P. Gillett (2014), Recent observed and simulated warming, *Nat. Clim. Change*, *4*, 150–151.

Goddard, L. (2014), Heat hide and seek, *Nat. Clim. Change*, *4*, 158–161.

González-Rouco, J. F., H. Beltrami, E. Zorita, and M. B. Stevens (2009), Borehole climatology: A discussion based on contributions from climate modeling, *Clim. Past*, *4*, 1–80.

Hansen, J., M. Sato, P. Kharecha, and K. von Schuckmann (2011), Earth's energy imbalance and implications, *Atmos. Chem. Phys.*, *11*, 13,421–13,449.

Hansen, J., et al. (2005), Earth's energy imbalance: Confirmation and implications, *Science*, *308*, 1431–1435.

Hansen, J., et al. (2013), Assessing "dangerous climate change": Required reduction of carbon emissions to protect young people, future generations and nature, *PLoS ONE*, *8*, e81648.

Harris, R. N., and D. S. Chapman (2001), Mid-latitude (30–60 n) climatic warming inferred by combining borehole temperatures with surface air temperatures, *Geophys. Res. Lett.*, *28*, 747–750.

Hu, Q., and S. Feng (2005), How have soil temperatures been affected by the surface temperature and precipitation in the Eurasian continent?, *Geophys. Res. Lett.*, *32*, L14711, doi:10.1029/2005GL023469.

Huang, S. (2006), 1851–2004 annual heat budget of the continental landmasses, *Geophys. Res. Lett.*, *33*, L04707, doi:10.1029/2005GL025300.

Huang, S., H. N. Pollack, and P. Y. Shen (2000a), Temperature trends over the past five centuries reconstructed from borehole temperatures, *Nature*, *403*, 756–758.

Huang, W., et al. (2000b), Seismic polarization anisotropy beneath the central Tibetan Plateau, *J. Geophys. Res.*, *105*, 27,979–27,989.

Jansen, E., et al. (2007), Palaeoclimate, in *Climate Change 2007: The Physical Science Basis. Contribution of Working Group I to the Fourth Assessment Report of the Intergovernmental Panel on Climate Change*, edited by S. Solomon et al., Cambridge Univ. Press, Cambridge, U. K., and New York.

Jaupart, C., and J.-C. Marechal (2011), *Heat Generation and Transport in the Earth*, Cambridge Univ. Press, New York.

Jones, P., et al. (2009), High-resolution palaeoclimatology of the last millennium: A review of current status and future prospects, *The Holocene*, *19*, 3–49.

Kosaka, Y., and S.-P. Xie (2013), Recent global-warming hiatus tied to equatorial pacific surface cooling, *Nature*, *501*, 403–407.

Lanczos, C. (1961), *Linear Differential Operators*, Van Nostrand, London.

Le Quéré, C., et al. (2014), Global carbon budget 2014, *Earth Syst. Sci. Data Discuss.*, *7*, 521–610.

Levitus, S., J. Antonov, and T. Boyer (2005), Warming of the world ocean, 1955–2003, *Geophys. Res. Lett.*, *32*, L02604, doi:10.1029/2004GL021592.

Levitus, S., et al. (2012), World ocean heat content and thermosteric sea level change (0–2000 m), 1955–2010, *Geophys. Res. Lett.*, *39*, L10603, doi:10.1029/2012GL051106.

Lewis, T. J. (1992), Climatic change inferred from underground temperatures, *Palaeogeogr. Palaeoclimatol. Palaeoecol.*, *98*, 78–282.

Luterbacher, J., et al. (2006), Mediterranean climate variability over the last centuries: A review, in *Mediterranean Climate Variability*, edited by P. Lionello, P. Malanotte-Rizoli, and R. Boscolo, Elsevier, Amsterdam.

Mareschal, J.-C., and H. Beltrami (1992), Evidence for recent warming from perturbed thermal gradients: Examples from Eastern Canada, *Clim. Dyn.*, *6*, 135–143.

Murphy, D. M., S. Solomon, R. W. Portmann, K. H. Rosenlof, P. M. Forster, and T. Wong (2009), An observationally based energy balance for the Earth since 1950, *J. Geophys. Res.*, *114*, D17107, doi:10.1029/2009JD012105.

Nitoiu, D., and H. Beltrami (2005), Subsurface thermal effects of land use changes, *J. Geophys. Res.*, *110*, F01005, doi:10.1029/2004JF000151.

Palmer, M. D., and D. J. McNeall (2014), Internal variability of Earth's energy budget simulated by CMIP5 climate models, *Environ. Res. Lett.*, *9*, 034016.

Phipps, S. J., et al. (2013), Paleoclimate data–model comparison and the role of climate forcings over the past 1500 years, *J. Clim.*, *26*, 6915–6936.

Pollack, H. N., and J. E. Smerdon (2004), Borehole climate reconstructions: Spatial structure and hemispheric averages, *J. Geophys. Res.*, *109*, D11106, doi:10.1029/2003JD004163.

Pollack, H. N., D. Y. Demezhko, A. D. Duchkov, I. V. Golovanova, S. Huang, V. A. Shchapov, and J. E. Smerdon (2003), Surface temperature trends in Russia over the past five centuries reconstructed from borehole temperatures, *J. Geophys. Res.*, *108*(B4), 2180, doi:10.1029/2002JB002154.

Pollack, H. N., J. E. Smerdon, and P. E. van Keken (2005), Variable seasonal coupling between air and ground temperatures: A simple representation in terms of subsurface thermal diffusivity, *Geophys. Res. Lett.*, *32*, L15405, doi:10.1029/2005GL023869.

Randall, D., et al. (2007), Climate models and their evaluation, in *Climate Change 2007: The Physical Science Basis. Contribution of Working Group I to the Fourth Assessment Report of the Intergovernmental Panel on Climate Change*, edited by S. Solomon et al., Cambridge Univ. Press, Cambridge, U. K., and New York.

Rath, V., J. González-Rouco, and H. Goosse (2012), Impact of postglacial warming on borehole reconstructions of last millennium temperatures, *Clim. Past*, *8*, 1059–1066.

Rhein, M., et al. (2013), Observations: Ocean, in *Climate Change 2013: The Physical Science Basis. Contribution of Working Group I to the Fifth Assessment Report of the Intergovernmental Panel on Climate Change*, Cambridge Univ. Press, Cambridge, U. K., and New York.

Roy, S., R. N. Harris, R. U. M. Rao, and D. S. Chapman (2002), Climate change in India inferred from geothermal observations, *J. Geophys. Res.*, *107*(B7), 2138, doi:10.1029/2001JB000536.

Santer, B. D., et al. (2014), Volcanic contribution to decadal changes in tropospheric temperature, *Nat. Geosci.*, *7*, 185–189.

Schmidt, G. A., D. T. Shindell, and K. Tsigaridis (2014a), Reconciling warming trends, *Nat. Geosci.*, *7*, 158–160.
Schmidt, G. A., et al. (2014b), Using palaeo-climate comparisons to constrain future projections in CMIP5, *Clim. Past*, *10*, 221–250.
Schmidt, H., et al. (2013), Response of the middle atmosphere to anthropogenic and natural forcings in the CMIP5 simulations with the Max Planck Institute Earth system model, *J. Adv. Model. Earth Syst.*, *5*, 98–116.
Schmidt, W. L., W. D. Gosnold, and J. W. Enz (2001), A decade of air–ground temperature exchange from Fargo, North Dakota, *Global Planet. Change*, *29*, 311–325.
Shen, P. Y., and A. E. Beck (1992), Paleoclimate change and heat flow density inferred from temperature data in the Superior Province of the Canadian Shield, in *Climatic Change Inferred From Underground Temperatures, Paleogeography, Paleoclimatology, Paleoecology (Global and Planetary Change Section)*, vol. 98, edited by T. J. Lewis, pp. 143–165, Elsevier, Amsterdam.
Smerdon, J. E., H. N. Pollack, J. W. Enz, and M. J. Lewis (2003), Conduction-dominated heat transport of the annual temperature signal in soil, *J. Geophys. Res.*, *108*(B9), 2431, doi:10.1029/2002JB002351.
Smerdon, J. E., H. N. Pollack, V. Cermak, J. W. Enz, M. Kresl, J. Šafanda, and J. F. Wehmiller (2004), Air-ground temperature coupling and subsurface propagation of annual temperature signals, *J. Geophys. Res.*, *109*, D21107, doi:10.1029/2004JD005056.
Smerdon, J. E., H. N. Pollack, V. Cermak, J. W. Enz, M. Kresl, J. Safanda, and J. F. Wehmiller (2006), Daily, seasonal and annual relationships between air and subsurface temperatures, *J. Geophys. Res.*, *111*, D07101, doi:10.1029/2004JD005578.
Smerdon, J. E., H. Beltrami, C. Creelman, and M. B. Stevens (2009), Characterizing land surface processes: A quantitative analysis using air-ground thermal orbits, *J. Geophys. Res.*, *114*, D15102, doi:10.1029/2009JD011768.
Solomon, S. (2007), *Climate Change 2007—The Physical Science Basis: Working Group I Contribution to the Fourth Assessment Report of the IPCC*, vol. 4, Cambridge Univ. Press, Cambridge, U. K., and New York.
Stieglitz, M., S. Déry, V. Romanovsky, and T. Osterkamp (2003), The role of snow cover in the warming of arctic permafrost, *Geophys. Res. Lett.*, *30*(13), 1721, doi:10.1029/2003GL017337.
Stocker, T., et al. (eds.) (2013), *Climate Change 2013: The Physical Science Basis. Contribution of Working Group I to the Fifth Assessment Report of the Intergovernmental Panel on Climate Change*, 1535 pp., Cambridge Univ. Press, Cambridge, U. K., and New York.
Sushama, L., R. Laprise, and M. Allard (2006), Modeled current and future soil thermal regime for northeast Canada, *J. Geophys. Res.*, *111*, D18111, doi:10.1029/2005JD007027.
Sushama, L., R. Laprise, D. Caya, D. Verseghy, and M. Allard (2007), An RCM projection of soil thermal and moisture regimes for North American permafrost zones, *Geophys. Res. Lett.*, *34*, L20711, doi:10.1029/2007GL031385.
Trenberth, K. E., and J. T. Fasullo (2013), An apparent hiatus in global warming?, *Earth's Future*, *1*, 19–32.
Vasseur, G., P. Bernard, J. V. de Meulebrouck, Y. Kast, and J. Jolivet (1983), Holocene paleotemperatures deduced from geothermal measurements, *Palaeogeogr. Palaeoclimatol. Palaeoecol.*, *43*, 237–259.
Wiggins, R. A. (1972), The general linear inverse problem: Implication of surface waves and free oscillations for earth structure, *Rev. Geophys.*, *10*, 251–285.